ACTA IMEKO
ISSN: 2221-870X
March 2023, Volume 12, Number 1, 1 - 8

Terahertz techniques for better hazelnut quality

Manuel Greco[1], Fabio Leccese[1], Emilio Giovenale[2], Andrea Doria[2]

[1] *Science Department, Università degli Studi "Roma Tre", Rome 00146, Italy*
[2] *Fusion and Nuclear Dept, ENEA, Frascati, Rome 00044, Italy*

ABSTRACT
In recent years, technological innovation has acquired a fundamental role in the agri-food sector, in particular in food quality control. The development of technology allowed to improve the quality of the food before it is placed on the market. Recently, non-invasive techniques such as those operating in the THz spectral band were applied to the field of food quality control.
In the laboratories of the ENEA centre in Frascati, close to Rome-Italy, has been developed a THz imaging system operating in reflection mode and an experimental setup able to measure both reflection and transmission of the samples in the frequency range between 18-40 GHz. With these two setups will distinguish rotten and healthy hazelnuts acquiring in real time both images of the fruit inside the shell by using the imaging system and the transmission data exploiting the 18-40 GHz system.

Section: RESEARCH PAPER

Keywords: Terahertz; imaging; transmissions; YIG; hazelnut

Citation: Manuel Greco, Fabio Leccese, Emilio Giovenale, Andrea Doria, Terahertz techniques for better hazelnut quality, Acta IMEKO, vol. 12, no. 1, article 29, March 2023, identifier: IMEKO-ACTA-12 (2023)-01-29

Section Editor: Francesco Lamonaca, University of Calabria, Italy

Received February 6, 2023; **In final form** February 24, 2023; **Published** March 2023

Corresponding author: Manuel Greco, e-mail: manuel.greco@uniroma3.it

1. INTRODUCTION

One of the pillars of food quality is food safety. Reducing the presence of pathogens and detecting toxins in food production is a key part of the food production chain. To achieve a high standard of food quality control, a series of methods aimed at initially selecting the product and then placing it on the market, are available.

One of the most used techniques in the field of food safety is X-ray imaging [1]-[3], but other methodologies such as ultrasound techniques [4], [5] also find space. One of the main advantages of x-ray techniques is that they produce high resolution images: X-rays can pass through matter undergoing an attenuation which depends, for example, on the type of material crossed. The higher the density of the material crossed, the more the rays are absorbed and the lower the amount of radiation transmitted. The latter contains information relating to the absorption of radiation, which can be used to obtain an image of the structure crossed.

At the same time, techniques that use x-rays as an investigative tool are subject to limitations: some materials, such as wood and glass, are weakly detected due to their low density.

An additional important factor that needs to be taken into consideration, when using techniques like these, is their ionizing nature. As known, x-radiation having a wavelength capable of interacting directly with the electrons of the orbitals, triggering ionizations and, therefore, modifications at a chemical level. Furthermore, X-ray techniques can involve risks both for the operator and for the sample itself, since the X-ray photon is capable to tear electrons from matter and, therefore, can alter the quality of the food.

In recent years, techniques operating in the terahertz frequency have appeared on the market and may potentially provide additional information to those obtained with traditional routine techniques. At present, imaging and terahertz spectroscopy techniques have been used in various fields, such as pharmaceutical industries [6], cultural heritage [7], aerospace industry [8] and finally precision agriculture [9], [10].

THz radiation, differently from infrared radiation, excites rotational and roto/vibrational transitions, so polar liquids such as water have a strong absorption in this spectral band. While on one hand this important feature could be exploited to quantify the water content in foods, on the other hand it makes it a limit [11].

As previously reported, unlike X-ray techniques, whose photons ionize matter, THz photons have a much lower energy. By exploiting this characteristic, THz radiation is unable to cause ionizations and, therefore, induce structural changes in biomolecules. Therefore, techniques operating in this band can

be considered safe for operators, but above all for the purposes of food quality.

In the food industry, THz imaging technologies have proven useful in detecting food contaminants [12], [13]. As reported in several studies, the presence of chemical products on foods can lead to the onset of pathologies in consumers and therefore constitute a potential risk. Recently, a group of researchers applied terahertz time-domain spectroscopy (THz-TD) to detect the presence of pesticides in food powders such as sticky rice, sweet potato, and lotus root [14], highlighting specific absorbance peaks ranged from 0.5 to 1.6 THz for some pesticides.

Foreign bodies can be a problem in food safety as well. In [15], a THz imaging system, operating in transmission mode, was applied to detect foreign bodies, such as stones, glass fragments and metal screws in chocolate bars. All these elements were visible in the THz images.

As previously reported, the potential that terahertz technologies can demonstrate in food analysis is enormous. This potential needs to be tested in the laboratory on a large number of samples, possibly combined with artificial intelligence.

In this study, THz measurements by using a 97 GHz imaging system and an experimental setup were made on healthy and rotten hazelnuts samples.

2. IMAGING TERAHERTZ SCANNER

These THz measures on healthy and rotten hazelnut were made by using a THz imaging scanner operating in reflection mode. Figure 1A shows this system with some components, Figure 1B, while a more detail description from a physical point of view is reported in [16].

This system mainly consists of a 97 GHz source, a directional coupler, a truncated waveguide, a laser triangulation system and a Schottky diode; this last used as detector of the radiation. The IMPATT (Impact Ionization Avalanche Transit-Time) diode, Figure 1C, operates at a fixed frequency of 97 GHz with an output power of 70 mW and it was used as source.

This diode is based on the avalanche effect. When a strong electric field is applied to a semiconductor or insulator, it can accelerate the free electrons present in the material. After having gained a certain amount of energy and impacting against the atoms of the material, these particles are able to induce ionizations, i.e., lead to the formation of other free electrons. In this way, at the end of this process called the avalanche effect, the number of electrons will be greatly increased.

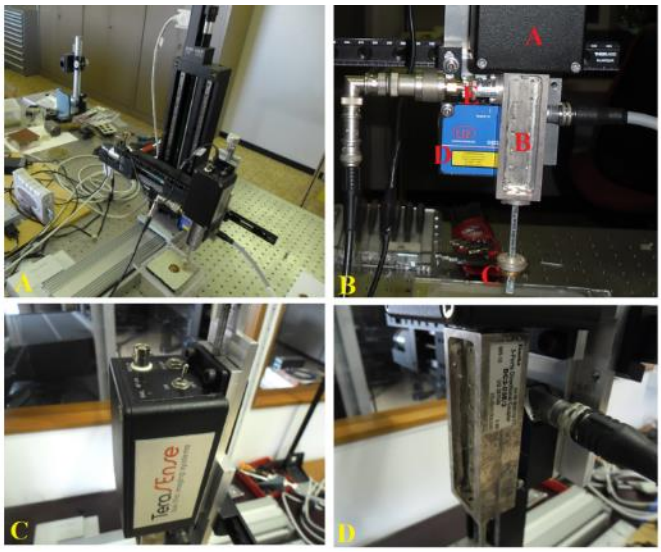

Figure 1 A. Imaging Terahertz System; 1 B. (A) source, (B) directional coupler, (C) truncated wave guide, (D) laser triangulation system and (E) Schottky diode; 1C. IMPATT diode at 97 GHz; 1D. Directional coupler.

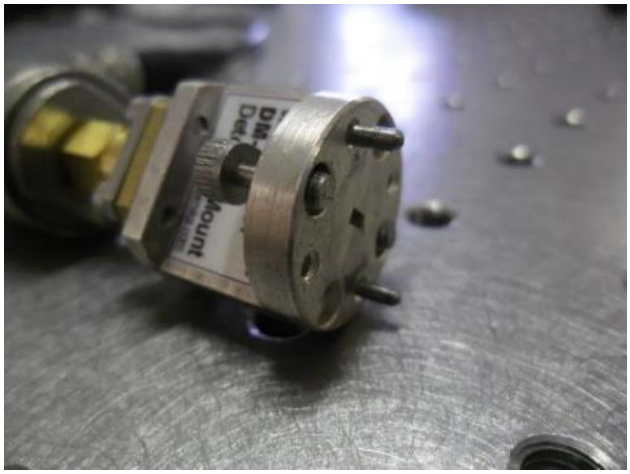

Figure 2. Schottky diode.

The IMPATT diode in this setup is connected to an Elmika three port directional coupler, based on WR-10 waveguide, with 3 dB attenuation as shown in Figure 1D. In this study, the directional coupler was used to collect a fraction of the signal reflected back by the sample.

A Schottky diode, shown in Figure 2, was used as detector of the radiation reflected. Thanks to this high switching speed, this diode can follow the oscillations of the electric field up to frequencies of the order of hundreds of GHz. In this imaging scanner, the voltage signal generated by the Schottky diode is sampled through an analogue-digital converter and sent to PC via USB interface.

It is advisable to be able to accurately measure the distance that separates the waveguide from the sample, both to be able to position it correctly and to be able to exploit the capabilities of the system to measure the phase of the reflected radiation. In fact, the phase value also depends on the distance travelled by the reflected radiation, and it is therefore crucial to be able to measure this distance accurately. In order to measure the distance between the waveguide and the sample, a laser triangulation system was used, see Figure 3.

Figure 3. Laser triangulation system.

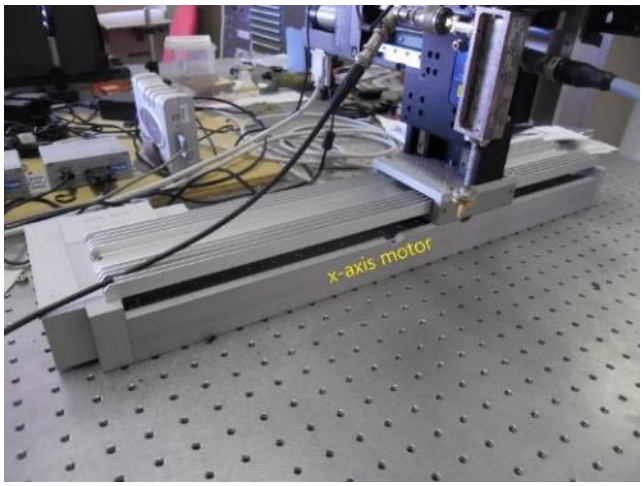

A

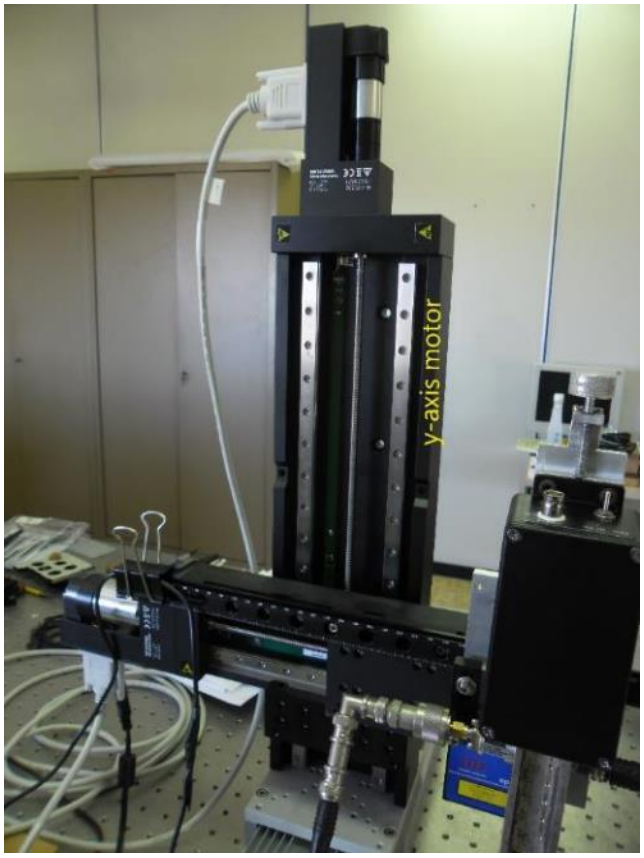

B

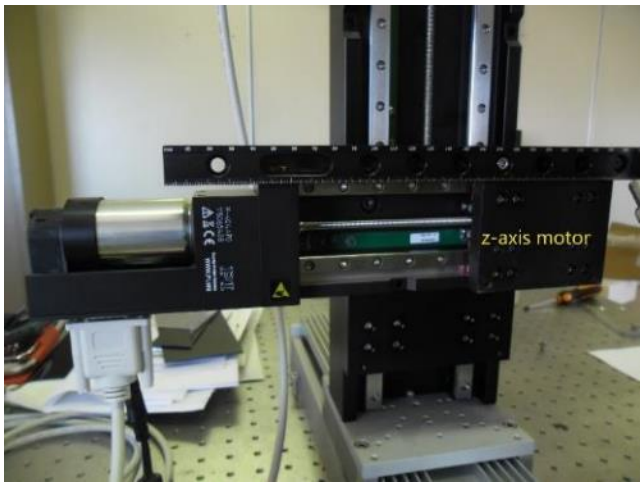

C

Figure 4. A. x-axis motor; 4 B. y-axis motor; 4 C. z-axis motor.

A laser diode emits a laser beam, which is projected onto the surface of the measurement target. Subsequently, once the beam has reached the sample, it will be reflected back to be subsequently captured by a CCD/CMOS sensor, positioned at a certain angle with respect to the optical axis of the laser beam. The target distance is calculated through a geometric algorithm, while the data is analysed by the internal or external controller and made available in output in different formats. In this work, the laser sensor had a wavelength of 670 nm, with an optical power of less than 1 mW and is capable of measuring distances between 50 and 100 mm with a resolution of 5 μm.

Furthermore, three stepper motors, Figure 4 A-B-C, have been used to move both the source and the detector along the three axes X, Y, Z. The movement of each motor is regulated by three mercury controllers.

The motors are controlled by suitable controllers that regulate all the motor parameters along the axis (X, Y, Z), translating the movement instructions sent via PC into electrical impulses which activate the physical movement of the motors. The three controllers are identical, but they are programmed by entering the parameters relating to the motor to be controlled (stroke, speed and acceleration characteristics, position of the reference probes, accuracy, etc.). The controllers can be connected to the control PC via USB port or RS232 interface.

3. 18-40 GHZ MEASUREMENT SYSTEM

This measurement system has been designed to measure the transmission of samples in the frequency range between 18 and 40 GHz. It is made up of an Yttrium Iron Garnet (YIG) source and a detector used to measure the power of the transmitted radiation. In order to easily measure, the interaction with the radiation takes place in free space, so it is necessary to launch the radiation with the appropriate horns. Then, the radiation emitted by the YIG source is propagated within a transmission line to the launching horn, and then collected, in this case via a horn, see Figure 5.

The transmitted signal is detected by means of a Schottky diode, and the voltage signal obtained is sent to a control PC via an analogue-digital converter also interfaced via a USB port.

Considering that each horn reflects a certain percentage of the radiation, the system consisting of the throwing horn, sample and horn used to collect the transmitted signal can be seen as a system composed of three partially reflecting mirrors. Each pair of mirrors in fact behaves like an interferometer, producing a series

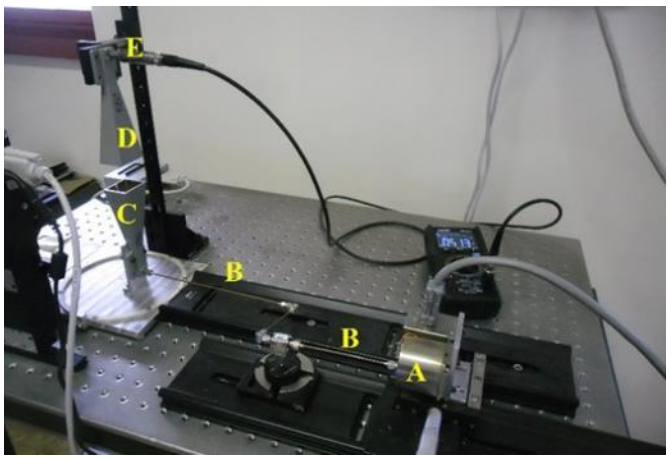

Figure 5. Image of the experimental setup. A) YIG Source; B) transmission line; C) launching horn; D) collecting horn; E) Schottky diode.

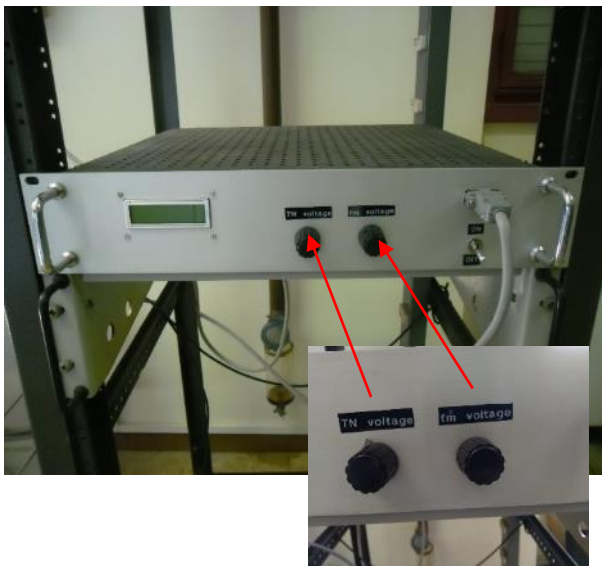

Figure 6. YIG driver system.

of effects, which allow to obtain information on the sample under examination.

This system, therefore, consists of a YIG driver system, a YIG source, a transmission line made with coaxial cables, a first horn used to launch the radiation, a second horn to collect the transmitted signal and a Schottky diode as detector.

The YIG driver system, shown in Figure 6, is able to drive the YIG oscillator MLOS-184 model.

On the front panel, 2 voltages, required for driving the YIG oscillator, are displayed. The main voltage (labelled with TN voltage on the display) powers the main coil and can be changed from 0 Volt to 10 Volts in continuous manner (according with Table 1 shown below). The fine voltage (labelled with fine modulation-fm coil voltage on the display) supplies power to the fine modulation coil allowing a little output frequency adjustment and can be changed from -10 V to 10 V.

At the ENEA centre in Frascati, close to Rome (Italy), a broadband YIG source was chosen, operating in the region between 18 and 40 GHz with a maximum power of about 20 mW. Figure 7 shows the YIG source used in this study.

Spinels, garnets and hexaferrites are among the most common magnetic oxides used in industry. Yttrium iron garnet is a synthetic crystal belonging to the garnet group. This material is used for tunable microwave electronic devices [17], circulators [18], insulators, phase shifters, tunable filters, and non-linear devices [19]. This crystal, also, can resonate at microwave

Table 1. Linear relationship between Voltage and frequency.

Tune Voltage (V)	Frequency (GHz)
0.00	18 GHz
1.00	20 GHz
2.00	22 GHz
3.00	24 GHz
4.00	27 GHz
5.00	29 GHz
6.00	31 GHz
7.00	33 GHz
8.00	36 GHz
9.00	38 GHz
10.00	40 GHz

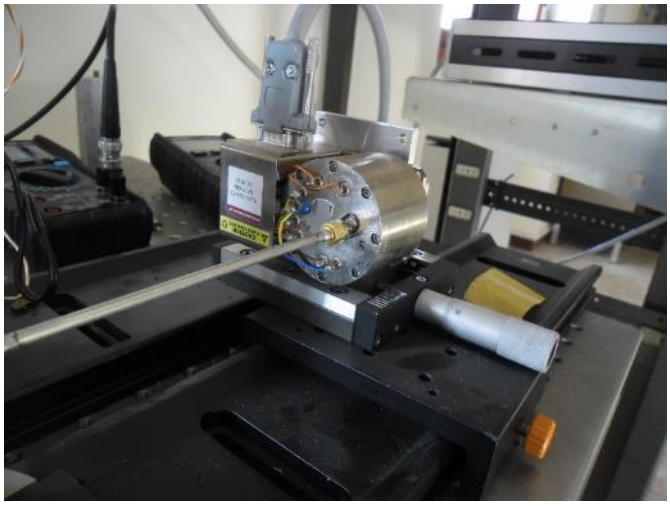

Figure 7. YIG source.

frequencies when it is immersed into a static magnetic field. This resonance frequency is directly proportional to the strength of the magnetic field applied to the crystal. The magnetic field can be generated using an electromagnet, a permanent magnet, or a combination of both. The magnetic field of an electromagnet can be tuned using a variable current, thus, by using this crystal, we are to make a tuneable frequency source.

A layer of eccosorb was placed inside the petri dish as shown in Figure 8. A hole having the same dimensions of the hazelnuts was created in the eccosorb layer to allow the radiation to pass only through the sample.

A Schottky diode was used to detect the transmitted signal through the sample, Figure 9.

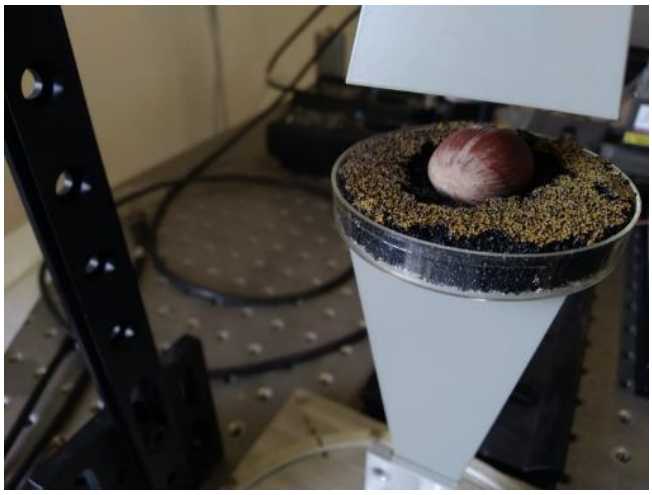

Figure 8. Petri dish with an eccosorb layer placed inside the dish itself.

Figure 9. Schottky diode

4. HAZELNUT SAMPLES

In this study, THz measurements were made on 5 healthy and 5 rotten hazelnuts belonging to the "Tonda Gentile Romana" species which together with the "Nocchione" are the most widespread species in Lazio and Central Italy, Figure 10. The Tonda Gentile Romana has a hazelnut colour with shiny dark brown streaks, a smell of toasted hazelnuts, a toasted hazelnut flavor with no bitter or rancid aftertaste and a spheroidal appearance.

Figure 10. Rotten and healthy hazelnuts.

5. RESULTS AT 97 GHZ

In order to carry out the measurements with the imaging system, the waveguide was positioned very close to the outer shell of each hazelnut.

Since the THz imaging system was designed to detect the phase shift of the reflected signal, by changing the distance that separates the sample from the waveguide by approximately 1.5 mm, corresponding to half a wavelength, this causes a phase shift, producing different coloured pixels in the image. In Figure 11A-B the visible and THz image of the first two healthy hazelnuts is shown.

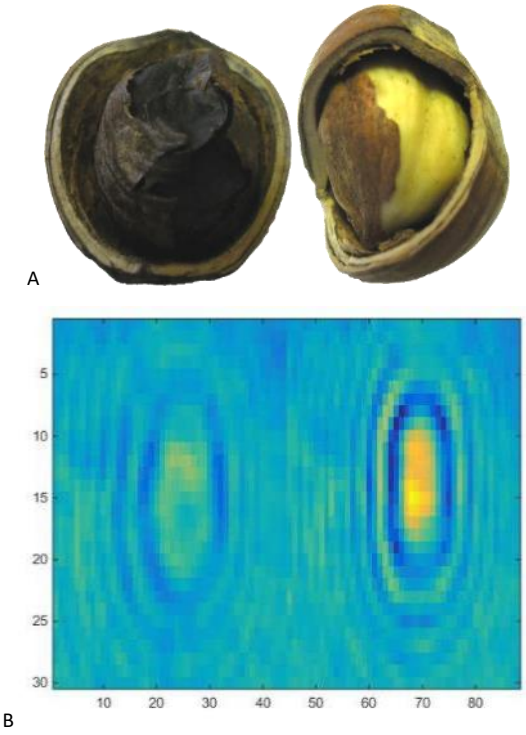

Figure 11. A. On the left, the first healthy hazelnut; on the right, the second healthy hazelnut. At first glance the first healthy one didn't seem rotten; 11 B. THz image of the first two healthy hazelnuts.

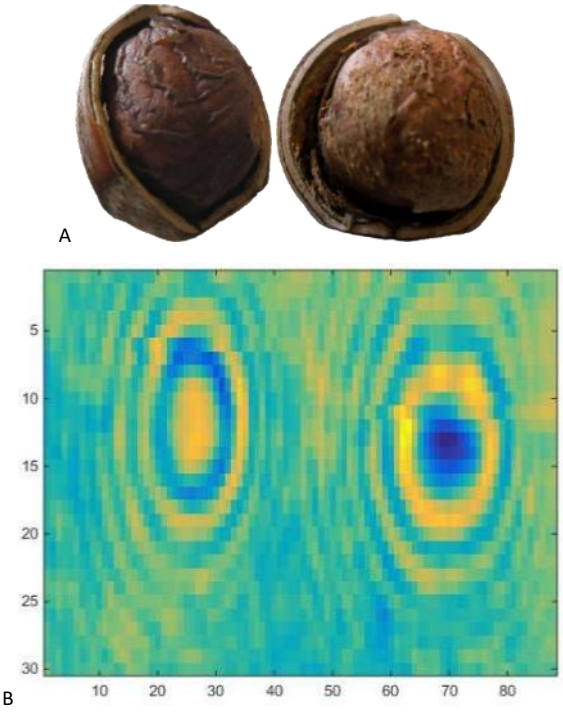

Figure 12. A. On the left, the third healthy hazelnut; on the right, the fourth healthy hazelnut; 12. B. THz images of the third and fourth healthy hazelnut.

The first healthy hazelnut at first glance did not seem rotten and showed no sign of deterioration, but breaking the outer shell the fruit was rotten. From the terahertz image can be seen that the fruit of the first healthy hazelnut does not have a well-defined, rounded shape if compared to the second healthy one. The second healthy hazelnut, contrarily, shows a well-defined shape. In Figure 12A-B the visible and THz image of the third and fourth healthy hazelnut are shown.

From the terahertz images can be seen that the fruit of the third and fourth healthy hazelnut has a rounded shape. The

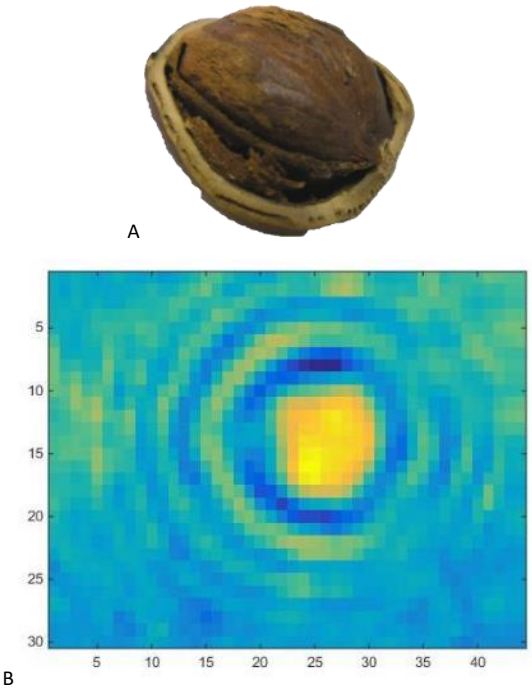

Figure 13. A. Visible image of the fifth healthy hazelnut; 13. B. THz image of the fifth healthy hazelnut.

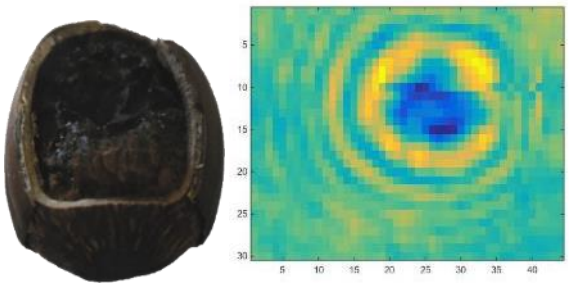

Figure 14. On the left, visible image of the first rotten hazelnut; on the right THz image of the rotten one.

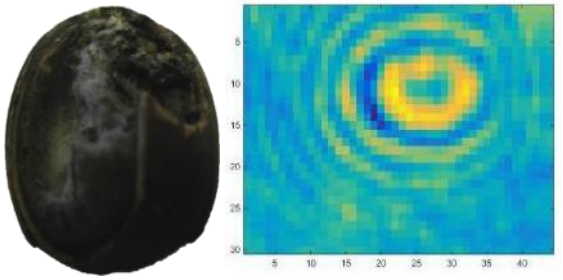

Figure 15. On the left, visible image of the first second rotten hazelnut; on the right, THz image of the rotten one.

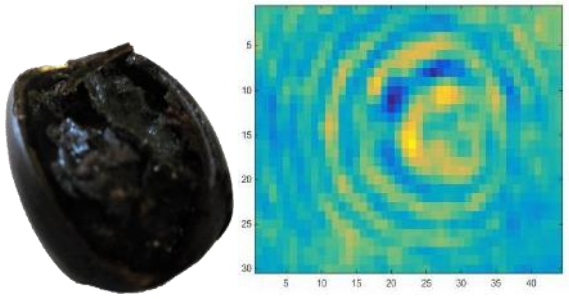

Figure 16. On the left, visible image of the third rotten hazelnut; on the right, THz image of the rotten one.

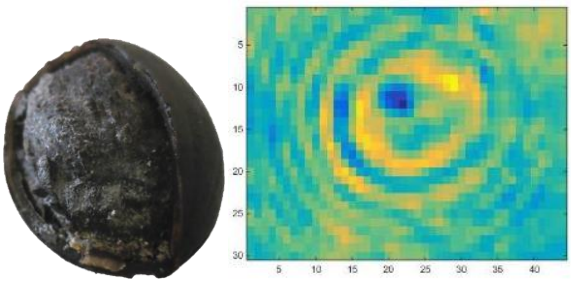

Figure 17. On the left, visible image of the fourth rotten hazelnut; on the right, THz image of the rotten one.

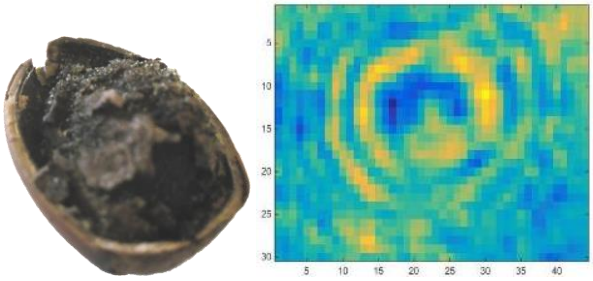

Figure 18. On the left, visible image of the fifth rotten hazelnut; on the right, THz image of the rotten one.

hazelnut shown on the left is coloured yellow while the one on the right is blue. This is explained by the fact that each hazelnut having a well-defined shape and therefore size, this phenomenon causes a phase shift from a physical point of view. Finally, in Figure 13A-B, the visible and terahertz image of the fifth healthy hazelnut are shown.

The same procedure was also followed for rotten hazelnuts. Figure 14, Figure 15, Figure 16, Figure 17, and Figure 18 show the visible and THz image of the rotten hazelnuts, respectively. From the THz images, the hazelnuts don't have a regular shape, i.e., rounded.

6. RESULTS AT 18-40 GHZ

After carrying preliminary tests, we realized that it is better to operate in the upper frequency limit of the emission range: when operating below 36 GHz, the diffractive effects due to the higher wavelength, comparable to the hazelnuts dimensions, produce results difficult to analyse, due to the high background radiation transmission.

Operating at shorter wavelength makes the system able to clearly distinguish between healthy and rotten hazelnuts. Focusing on the frequency range between 36 and 40 GHz, with a wavelength range between 8 and 7 millimetres, smaller than the size of hazelnuts, better results were obtained. To test the new setup, we decided to examine five healthy hazelnuts and five rotten ones by modulating the voltage between 8 and 10 Volts. In the graph in Figure 19, the transmission values relating to healthy and rotten hazelnuts are shown.

In Figure 19, in each series of data, corresponding to a specific frequency, the transmission of the healthy hazelnuts is shown at

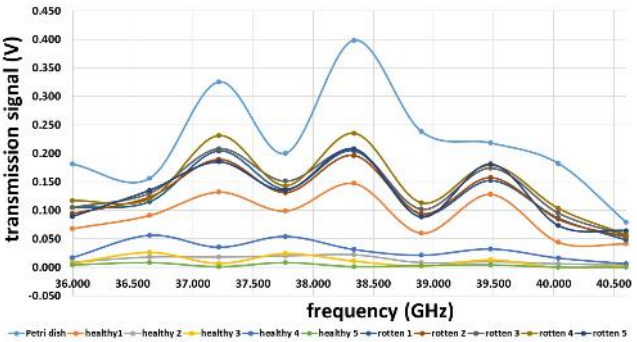

Figure 19. Measures performed at different frequencies, corresponding to applied voltages between 8 V and 10 V.

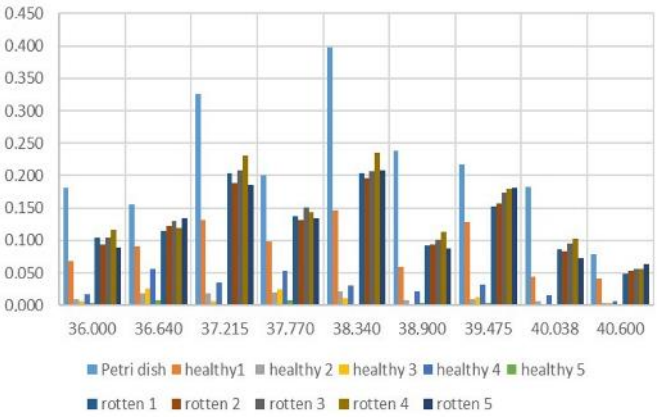

Figure 20. The orange bar highlights the transmission relating to the first healthy hazelnut.

Figure 21. First healthy hazelnut external visual inspection and status of the inner fruit (degraded).

the bottom of the graph while the one referring to the rotten is shown above. From the graph, the highest transmission values are those relating to the Petri dish used as baseline.

A clear difference in transmission between healthy and rotten hazelnuts is evident, apart from the data from the first nut (orange bar in the graph in Figure 20), that shows a transmission comparable to that of the rotten hazelnuts. The lower transmission of the healthy hazelnuts is correlated to the higher amount of fatty acids, which absorb the radiation.

The anomaly of the first sample gave us a confirmation of this principle and of its possible practical application as a discrimination tool to identify rotten hazelnuts. Sample 1 didn't show, on visual inspection, any sign of deterioration, but when the outer shell was broken, the fruit was rotten as shown in Figure 21.

This is a clear demonstration that this system is able to identify hazelnuts that would be judged "healthy" as well on the basis of a simple visual inspection (that is the most used method in practice) and demonstrates the absence of any bias in the experiment.

7. CONCLUSIONS

From this study, we have seen how the THz reflection imaging system and the 18-40 GHz experimental system have proved to be non-destructive tools in the food industry. As reported in several scientific papers, terahertz techniques have been used to detect pesticides, fertilizers, and moisture in food. Despite these advantages, the technique currently has some limitations, mainly related to its possible use in its practical use in an industrial environment.

The terahertz imaging system has shown the capability of differentiating hazelnuts, but at the same time it presents some limitations, the main one of which is given by the scan time required to acquire a single hazelnut (30 seconds to scan a hazelnut), which is too long for a possible application in a production line. A possible solution could be to modify the layout of the instrumentation to carry out the measures in transmission mode, exploiting a THz-sensitive matrix detector, for one-shot image acquisition.

To reduce the scanning time, it was therefore thought to design a device operating in transmission by detecting the signal transmitted through the nut. This device is also able to operate in a frequency range between 18 and 40 GHz thanks to the YIG source used for this purpose. So, by modulating the magnetic field applied to the yttrium-iron garnet we are able to select the resonance frequency of the crystal. Furthermore, this experimental system compared to the THz imaging system is cheaper and faster in terms of data acquisition. Finally, from the acquired data it was possible to detect hazelnuts, which at first sight seemed healthy but were rotten.

REFERENCES

[1] H. Einarsdóttir, M. J. Emerson, L. H. Clemmensen, K. Scherer, K. Willer, M. Bech, R. Larsen, B. K. Ersbøll, F. Pfeiffer, Novelty detection of foreign objects in food using multi-modal X-ray imaging, Food Control, 67, pp. 39-47. DOI: 10.1016/j.foodcont.2016.02.023

[2] R. P. Haff, N. Toyofuku, X-ray detection of defects and contaminants in the food industry, Sensing and Instrumentation for Food Quality and Safety, 2(4), pp. 262–273. DOI: 10.1007/s11694-008-9059-8

[3] M. S. Nielsen, T. Lauridsen, L. B. Christensen, R. Feidenhans'l, Xray dark-field imaging for detection of foreign bodies in food. Food Control, 30(2), pp. 531–535. DOI: 10.1016/j.foodcont.2012.08.007

[4] J. Chandrapala, C. Oliver, S. Kentish, M. Ashokkumar, Ultrasonics in food processing - food quality assurance and food safety, Trends in Food Science and Technology, 26(2), pp. 88-98. DOI: 10.1016/j.tifs.2012.01.010

[5] B. Zhao, Y. Jiang, O. A. Basir, G. S. Mittal, Foreign body detection in foods using the ultrasound pulse/echo method: Foreign body detection in Thoughout foods, Journal of Food Quality, 27(4), pp. 274–288. DOI: 10.1111/j.1745-4557.2004.00651.x

[6] D. M. Charron, K. Ajito, J. Kim, Y. Ueno, Chemical mapping of pharmaceutical cocrystals using terahertz spectroscopic imaging, Analytical Chemistry, 85 (4), pp. 1980-1984. DOI: 10.1021/ac302852n

[7] A. Doria, G. P. Gallerano, E. Giovenale, M. Greco, M. Picollo, THz detection of water: Applications on mural paintings and mosaics, Proc. of the 42nd Int. Conf. on Infrared, Millimeter, and Terahertz Waves, IRMMW-THz, Cancun, Mexico, 27 August-1 September 2017, pp. 1-2. DOI: 10.1109/IRMMW-THz.2017.8067164

[8] M. Greco, E. Giovenale, F. Leccese, A. Doria, E. De Francesco, G. Piero Gallerano, A THz imaging scanner to detect structural and fire damage on glass fiber composite, Proc. of the IEEE 9th International Workshop on Metrology for AeroSpace, MetroAeroSpace, Pisa, Italy, 27-29 June 2022, pp. 384-389. DOI: 10.1109/MetroAeroSpace54187.2022.9856003

[9] M. Greco, E. Giovenale, F. Leccese, A. Doria, A discrimination of healthy and rotten hazelnuts using a THz imaging scanner, Proc. of the IEEE Workshop on Metrology for Agriculture and Forestry, MetroAgriFor, Perugia, Italy, 3-5 November 2022, pp. 229-233. DOI: 10.1109/MetroAgriFor55389.2022.9964672

[10] M. Greco, E. Giovenale, F. Leccese, A. Doria, E. De Francesco, G. P. Gallerano, A THz imaging scanner to monitor leaf water content, Proc. of the IEEE Int. Workshop on Metrology for Agriculture and Forestry, MetroAgriFor, Trento-Bolzano, Italy, 3-5 November 2021, pp. 7-11. DOI: 10.1109/MetroAgriFor52389.2021.9628522

[11] A. A. Gowen, C. O'Sullivan, C. P. O'Donnell, Terahertz time domain spectroscopy and imaging: Emerging techniques for food process monitoring and quality control, Trends in Food Science and Technology, 25(1), pp. 40-46. DOI: 10.1016/j.tifs.2011.12.006

[12] M. Caciotta, S. Giarnetti, F. Leccese, B. Orioni, M. Oreggia, C. Pucci, S. Rametta, Flavors mapping by kohonen network classification of panel tests of extra virgin olive oil, Measurement: Journal of the International Measurement Confederation, 78, 2016, pp. 366-372. DOI: 10.1016/j.measurement.2015.09.051

[13] H. J. Shin, S. Choi, G. Ok, Qualitative identification of food materials by complex refractive index mapping in the terahertz range, Food Chemistry, 245, pp. 282-288. DOI: 10.1016/j.foodchem.2017.10.056

[14] A. Ren, A. Zahid, D. Fan, X. Yang, M. A. Imran, A. Alomainy, Q. H. Abbasi, State-of-the-art in terahertz sensing for food and water security – A comprehensive review, Trends in Food Science and Technology, 85, pp. 241-251.
DOI: 10.1016/j.tifs.2019.01.019

[15] G. Ok, H. J. Kim, H. S. Chun, S. Choi, Foreign-body detection in dry food using continuous sub-terahertz wave imaging, Food Control, 42, pp. 284-289.
DOI: 10.1016/j.foodcont.2014.02.021

[16] A. Doria, G. P. Gallerano, E. Giovenale, L. Senni, M. Greco, M. Picollo, C. Cucci, K. Fukunaga, A. C. More, An alternative phase-sensitive THz imaging technique for art conservation: History and new developments at the ENEA center of Frascati, Applied Sciences (Switzerland), 10(21), pp. 1-24.
DOI: 10.3390/app10217661

[17] C.-W. Nan, M. I. Bichurin, S. Dong, D. Viehland, G. Srinivasan, Multiferroic magnetoelectric composites: Historical perspective, status, and future directions, Progress in advanced dielectrics, pp. 191-293.
DOI: 10.1142/9789811210433_0005

[18] J. Ganne, R. Lebourgeois, M. Paté, D. Dubreuil, L. Pinier, H. Pascard, The electromagnetic properties of cu-substituted garnets with low sintering temperature, Journal of the European Ceramic Society, 27(8-9) 2007, pp. 2771-2777.
DOI: 10.1016/j.jeurceramsoc.2006.11.054

[19] J. D. Adam, L. E. Davis, G. F. Dionne, E. F. Schloemann, S. N. Stitzer, Ferrite devices and materials, IEEE T. Microw. Theory. 50 (2002), pp. 721-737.
DOI: 10.1109/22.989957